JOURNAL OF MARITIME RESEARCH

Vol XXIII. No. II (2026) pp 194–201

ISSN: 1697-4840, www.jmr.unican.es

A Comparative Hydrodynamic Analysis of the CS50 MK II and a Traditional Semisubmersible in the Bay of Bengal

Mir Tareque Ali[1,*], Md. Samiul Basir[2]

ARTICLE INFO

Article history:
Received 25 Jun 2025;
in revised form 11 Jul 2025;
accepted 01 Aug 2025.

Keywords:
Hydrodynamic analysis, Semi-submersible, Motion response, Mooring system, CS50 MK II, Bay of Bengal.

ABSTRACT

Due to the discovery and extraction of large amounts of gas by neighboring countries India and Myanmar in the offshore area, Bangladesh, with similar geology in the Bay of Bengal, should make a rapid move to boost its offshore oil and gas exploration in order to strengthen its economy. In shallow waters, fixed structures are preferred for oil and gas extraction. However, in deep waters, fixed structures are not feasible, making floating semisubmersibles the most effective solution for oil and gas extraction. This study presents a numerical analysis of the motion responses of moored semisubmersibles in the Bay of Bengal, comparing the CS50 MK II – a highly efficient and widely adopted design - with a traditional four-column semisubmersible. Both frequency domain and time domain analyses were performed, incorporating specific wave characteristics and current conditions at the study location. While there is no definitive conclusion on which design performs better, this work may provide a foundational understanding, guiding the ongoing improvement and innovation in semisubmersible platform design and deployment in the Bay of Bengal.

1. Introduction.

Currently Bangladesh is in the eighth position with a population size of about 175 million with a land area of about 130170 sq. km., as reported by the world population review. With a rapidly growing population and significant infrastructural developments, the country requires a continuous energy supply to meet the demands of its increasing need for energy and power [1].

The total no. of gas fields discovered in Bangladesh is 29 and the proven reserve is 28.79 trillion cubic feet (TCF). Until June 2023, a total of 20.33 TCF gas has been extracted, leaving only 8.46 TCF in the reserve. Out of 29 gas fields, only 20 gas fields are currently in operation delivering 2,300 million cubic feet of gas per day (MMCFD) against the current national demand of 3500 MMCFD [2]. The main reason behind the perilous situation in the gas sector is that in the last two decades, no significant gas fields were discovered. To mitigate the present crisis of gas demand in various sectors within this country, the government of Bangladesh decided to import Liquefied Natural Gas (LNG) from abroad spending valuable foreign currencies. Since 2018, an additional supply of 1000-1100 MMCFD in the national grid from the two floating storage regasification units (FSRUs) when both are in service. Considering the increase in demand of the gas supply in future, the total scenario looks very ominous for our country. Therefore, we are left with no other choice but to go for exploration for gas resources in the Bay of Bengal. Our maritime area is increased by 118113 sq. km. after the settlement of maritime disputes with its two neighboring countries Myanmar and India in 2012 and 2014 respectively [3]. According to the opinion of various experts in the petroleum engineering field, there is a tremendous prospect of a massive gas reserve in the Bay of Bengal, especially when we consider the exploration of gas by our neighboring countries

[1]Professor, Department of Naval Architecture & Marine Engineering, Bangladesh University of Engineering & Technology, Dhaka–1000, Bangladesh.

[2]Student, Department of Naval Architecture & Marine Engineering, Bangladesh University of Engineering & Technology, Dhaka–1000, Bangladesh.

[*]Corresponding author: Mir Tareque Ali. E-mail Address: mtarequeali@name.buet.ac.bd.

India and Myanmar. A total of around 40 TCF gas has been discovered by India, where as our another neighboring country Myanmar has also discovered 3 gas fields from 2003 to 2006 totaling a reserve of 6 TCF to 10 TCF gas in the Bay of Bengal [4]. Out of our 24 shallow water and deep sea blocks with the Bay of Bengal almost 90% of these offshore blocks are yet to be explored.

A number of different types of offshore structures have been operated world-wide for various purposes in a varying depth of water. Offshore structures to extract hydrocarbon resources like oil and gas can be broadly divided into fixed and floating types. Fixed offshore structures are usually suitable for shallow water depth up to 150 m, however floating offshore structures have emerged as the preferred option for deep-water operations. In the maritime industry, the semisubmersible type floating offshore structures are becoming increasingly popular for deeper waters due to its important design features like stability in high sea conditions, high mobility, good motion response characteristics, large working space etc. In order to operate these types of semisubmersible floating structures in the Bay of Bengal amid the challenging environmental conditions, including frequent cyclones, heavy rainfall (ranging from approximately 1000 mm to over 3000 mm), seismic activity, strong currents (sometimes exceeding 1.5 m/s), and varying water depths (deep basins exceeding 4000 meters), numerical simulation results for motion responses can be helpful for the selection design selection of these type of structures.

Offshore structures vary significantly based on their use and water depth. Sarhan and Raslan [5] emphasize that jacket platforms are cost-effective for shallow waters but impractical for deep and ultra-deep waters, requiring alternative solutions. Ruzanna [6] advocates for six-column twin pontoons over traditional four-column semi-submersibles in deepwater, citing enhanced stability and performance.

Ralha et al. [7] compare mooring systems for ultra - deepwater applications, noting the 12-line system's superior stability in depths of 2000m to 3000m. Patra et al. [8] introduce a numerical multi-scale nested modeling approach to study wave attributes in the Bay of Bengal, aligning predictions closely with buoy data near the Digha coast.

The hydrodynamic performance of semi-submersibles is influenced by waves, wind, and currents. Wu et al. [9] developed an algorithm for evaluating hydrodynamic performance under high sea states. Ng and Tahar [10] found that bidirectional waves significantly impact semi-submersible responses. Qiao and Ou [11] analyzed the global responses of semi-submersibles with different mooring systems in the South China Sea. Chuang et al. [12] optimized an arctic semi-submersible's dynamic performance using Potential Flow Theory and the Morison Equation. Alimuddin and Islam [13] compared HydroStar simulations of semi-submersibles in deep-sea regions of Bangladesh with published experimental data.

Mooring systems are crucial for the stability of a semisubmersible structure. Qiao and Ou [11] explored mooring line systems with buoys, reducing weight and radius in deep water. Liu et al. [14] studied the interaction between semi-submersibles and mooring systems using naoe-FOAM-SJTU. Zan et al. [15] developed advanced prediction models for mooring tension. Uwihanganye et al. [16] highlighted the importance of predicting mooring line damping accurately. Sanni and Olusegun [17] compared mooring systems for offshore vessels, providing design criteria using OrcaFlex.

Motion responses under different conditions have been extensively studied. Zhao et al. [18] used VIM-FOAM-SJTU for numerical simulations of vortex-induced motions (VIM) at various current headings. Hamn-Ching and Li [19] used the LES model to simulate deep-draft semi-VIM in currents at 45° angles. Vamshikrishna and Rajiv [20] experimentally studied VIM responses of a moored semi-submersible with and without a catenary riser. Rodolfo and Hamza [21] examined VIM in semi-submersibles with four square columns, focusing on the effects of headings and hull appendages. Yongpyo and Hanseong [22] tested a deep-draft semi-submersible's global motion in wind, wave, and current environments, noting significant VIM effects dependent on current speed and wave particle velocity.

Agroza et al. [23] studied offshore facilities for hydrate extraction in the Bay of Bengal, considering sedimentation and water depth for platform selection. Ove and Daniel [24] evaluated floating structural production concepts and associated riser systems for ultra-deep waters on India's east coast. Sarhan and Raslan [5] noted jacket platforms are cost-effective for shallow waters, while Ruzanna [6] suggested six-column twin pontoons are better suited for deep waters. Ralha et al. [7] highlighted the 12-line system's effectiveness in ultra-deep water, and Patra et al. [8] validated their wave model with real-world data from the Bay of Bengal.

The literature reveals significant advancements in understanding semi-submersibles' hydrodynamic performance, mooring systems, and motion responses. Current research emphasizes numerical simulations and experimental studies to optimize design and operational efficiency. There is a need for more comprehensive studies integrating real-world data with numerical models to enhance prediction accuracy. This research work investigates the numerical simulations of motion responses for moored semi-submersibles, specifically comparing the CS50 MK II [25] with a conventional four-column semi-submersible. The Moss CS-series catamaran platform has emerged as a highly successful and widely adopted design in the offshore industry over the past 20 years. The CS50 platforms were designed for dynamic positioning (DP) operations in challenging deepwater environments, supporting dual operations and high - capacity drilling systems. The analysis focuses on understanding the impact of these structures' design and mooring configurations under the unique wave and current conditions of the Bay of Bengal.

2. Mathematical Formulation of the Problem.

2.1. Assumptions and Coordinate Systems.

The motion response of a semi-submersible structure in the frequency domain can be formulated using potential flow theory and linear wave-body interaction principles. The body is subjected to small amplitude oscillations in water of uniform depth, induced by long-crested regular waves. Consider a three-dimensional body of arbitrary shape, freely floating in water, where the fluid is assumed to be incompressible, inviscid, and irrotational.

To analyze the dynamic behavior of a floating offshore structure in water waves, two Cartesian coordinate systems are employed as shown in Fig. 1. The first coordinate system is an earth fixed coordinate system ($o_E - x_E y_E z_E$) with the $o_E - x_E y_E$ plane representing the undisturbed mean free water surface and the z_E axis pointing vertically upwards. The earth-fixed system is fixed with respect to the earth and used to describe external forces acting on the ship. Another coordinate system, the body-fixed coordinate system ($o_B - x_B y_B z_B$) with the $o_B - x_B y_B$ plane representing the undisturbed mean free water surface and the z_B axis pointing vertically upwards. When the floating body is in its equilibrium position, the z_B axis passes through the body's centre of mass. The body-fixed system moves with the ship as it undergoes various motions (surge, sway, heave, roll, pitch, yaw) and used for defining hydrodynamic forces and ship responses in a moving reference frame. These coordinate definitions are essential for numerical simulations, ship stability assessments, and mooring analysis.

2.2. *Velocity Potentials.*

In regular waves, the linear potential ∅, which depends on both space and time, can be expressed as the product of a space-dependent term and a harmonic time dependent term as follows:

$$\phi(x, y, z; t) = \Re\left[\varphi(x, y, z)\, e^{-i\omega t}\right] \tag{1}$$

where $\varphi(x, y, z)$ is time independent quantity and the potential function $\varphi(x, y, z)$ can be separated into contributions from all modes of motion of the bodies and from the incident and diffracted wave fields as follows:

$$\varphi = -i\omega\left[(\varphi_0 + \varphi_7)\,\zeta_a + \sum_{j=1}^{6} \eta_j \varphi_j\right] \tag{2}$$

where φ_0 is the incident wave potential, φ_7 is the diffraction wave potential, φ_j represent potentials due to motion of the body in the j-th mode i.e., radiation wave potentials, η_j is the motion of the body in j-th mode, and ζ_a is the incident wave amplitude.

The incident wave potential can be expressed as:

$$\varphi_0 = \frac{g}{\omega^2} \frac{\cosh[k(z + h)]}{\cosh(kh)} e^{ik(x\cos\beta + y\sin\beta)} \tag{3}$$

where β is the angle of incident wave relative to the positive x-axis, h is the depth of water, g is the acceleration due to gravity and k is the wave number. The individual potentials are the solutions of Laplace equation and they need to satisfy the boundary conditions. According to the 3-D source distribution method, the potentials φ_7 and φ_j can be expressed in terms of well-known Green functions and as a result, boundary conditions are reduced to only on the wetted surfaces of the bodies [26].

Figure 1: Definition of coordinate system for the floating body in regular waves.

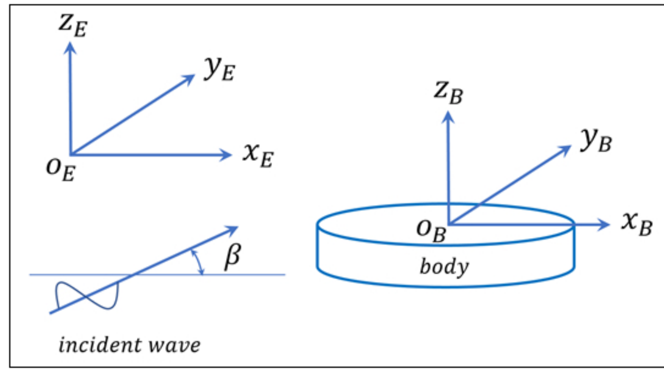

Source: Authors.

2.3. *Source Density and Green's Function.*

The potential function at some point (x, y, z) in the fluid region in terms of source distribution can be written as:

$$\varphi_j(x, y, z) = \frac{1}{4\pi} \iint_{S_B} \sigma_j(\xi, \eta, \zeta)\, G(x, y, z; \xi, \eta, \zeta)\, dS \qquad j = 1, 2, 3, \ldots, 7 \tag{4}$$

where $G(x, y, z; \xi, \eta, \zeta)$ denotes the Green's function of a source, singular in (ξ, η, ζ) and $\sigma_j(\xi, \eta, \zeta)$ is the complex source strength. Since Green's function satisfies the boundary conditions, applying the kinematics boundary condition on the immersed surface yields the following integral equation:

$$\frac{\partial \varphi_j(x, y, z)}{\partial n} = -\frac{1}{2}\sigma_j(x, y, z) + \frac{1}{4\pi} \iint_{S_B} \sigma_j(\xi, \eta, \zeta) \frac{\partial G(x, y, z; \xi, \eta, \zeta)}{\partial n}\, dS \qquad j = 1, 2, 3, \ldots, 7 \tag{5}$$

2.4. *Hydrodynamic Coefficients.*

Based on the linearized Bernoulli's equation, the hydrodynamic pressure distribution can be calculated by the following equation,

$$p = -\rho \frac{\partial \phi}{\partial t} = \rho\omega^2\left[(\varphi_0 + \varphi_7)\zeta_a + \sum_{j=1}^{6} \eta_j \varphi_j\right] e^{-i\omega t} \tag{6}$$

The first order wave exciting forces and moments in the k-th mode on the floating body can be written as follows:

$$F_k = -\rho\omega^2 \zeta_a\, e^{-i\omega t} \int_{S_B} (\varphi_0 + \varphi_7)\, n_k\, dS \tag{7}$$

The added mass and damping co-efficient can be expressed respectively as follows:

$$a_{kj} = -\Re\left[\rho \iint_{S_B} \varphi_j\, n_k\, dS\right] \tag{8}$$

$$b_{kj} = -\Im\left[\rho\omega \iint_{S_B} \varphi_j \, n_k \, dS\right] \tag{9}$$

2.5. *Equation of Motions.*

Upon solving the exciting forces, added mass coefficients, damping coefficients, the equations of six rigid body motions in the frequency domain can be written as:

$$\sum_{j=1}^{6} \left(M_{kj} + a_{kj}\right)\ddot{\eta}_j + b_{kj}\dot{\eta}_j + c_{kj}\eta_j = F_k$$
$$k = 1, 2, \ldots, 6$$

where M_{kj}, a_{kj}, b_{kj}, c_{kj} are the body inertia matrix, added mass coefficient matrix, damping matrix and hydrodynamic restoring matrix respectively in k^{th} mode due to motion in j^{th} mode, η_j is the vector containing translational and rotational oscillations about the co-ordinate axes and F_k is the wave exciting force matrix.

The equation of motion in time domain can be written as:

$$\sum_{j=1}^{6} \left[(M_{kj} + m_{kj})\ddot{x}_j(t) + \int_{-\infty}^{t} K_{kj}(t-\tau)\,\dot{x}_j(\tau)\,d\tau + C_{kj}x_j(t)\right] = F_{\text{wave},k}(t) + F_{\text{moor},k}(t) \tag{10}$$

where $k = 1, 2, \ldots.6$, M_{kj} is the inertia coefficient, m_{kj} is the frequency-independent added mass coefficient, K_{kj} is the retardation function, C_{kj} is the hydrostatic restoring force coefficient. $\ddot{x}$, $\dot{x}$ and x are the acceleration, velocity and displacement of the floating structure. $F_{wave,k}(t)$ is the wave exciting force, $F_{moor,k}(t)$ is the reaction force of the mooring lines.

3. Methodology.

3.1. *Model Parameter.*

In the present investigation, a traditional semisubmersible with four columns symmetric to x and y axis and CS50 MK II which has a six columns and catamaran shape pontoon is chosen. Both designs are selected for analysis as they have similar draft and displacement characteristics. The CS50 MK II 3D design is available in the Open source website GrabCad by RuneB [27]. The general specifications of both the semisubmersibles are presented in Table1.

3.2. *Mooring Configuration.*

The mooring system consist of a combination of conventional wire-chain system with 12 mooring lines described in Table 2 and Table 3. At the studied water depth, the fairlead component is 95 mm wire rope and the ground component is 84 mm stud link chain. The mooring system is balanced with 150 tons of pre-tension on fairlead as shown in Fig. 2.

3.3. *Block Selection and Wave Spectrum.*

The conventional integrated parameters, such as significant wave height (SWH) and mean wave period (MWP), offer limited insights into the concurrent presence of diverse wave systems. So, wave spectrum proposed by Patra et al. [8] is used as the irregular wave for the present study as presented in Fig. 3. Patra et al. [8] also conducted their study in 16 different locations, where the highest water depth is 1657 m close to Myanmar border. The specific location of co-ordinate (91.50°E, 19.60°N) as shown in Fig. 4 is chosen as it is close to Myanmar border, where survey has already been conducted by TGS-Schlumberger and a large amounts of gas field has been discovered.

Table 1: General specifications of the semisubmersibles.

	CS50 MK II	Traditional Semisubmersible with 4 Columns
	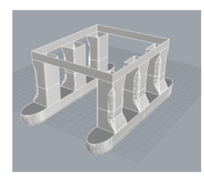	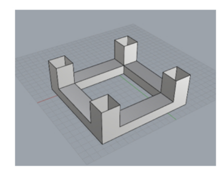
LOA	118 m	82.7 m
Breadth	73 m	82.7 m
Operating Draft:	23.5 m	23.5 m
Transit Draft	9.75 m	N/A
COG underwater:	15 m downwards from Water Surface	16.6 m downwards from Water Surface
Volume Displacement:	47042.14 m³	47042.14 m³
Column Width	14.9 m	15.2 m
Pontoon Height	16.3 m	9 m

Source: Authors.

Figure 2: 12-line mooring system configurations for the semisubmersibles.

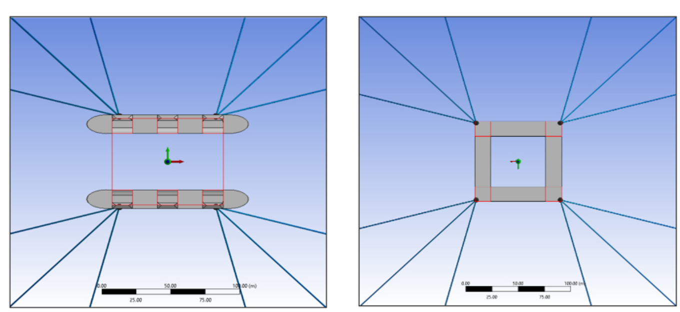

Source: Authors.

Table 2: Chain-wire rope mooring system properties.

Chain/Wire	Wet Weight (kg/m)	Elasticity EA (mT)	Breaking Strength (mT)
95mm Wire Rope	36	47037	810
84mm R5 Rig Chain	130	56444	828

Source: Authors.

Table 3: Chain-wire rope mooring system configurations.

Horizontal Distance (m)	Tension at the Fairlead (t)	95mm Wire Rope Length	84mm R5 Studlink Chain Length
2500	150 (mT)	~2520m	800 m

Source: Authors.

Figure 3: Wave spectrum for (91.50°E, 19.60°N) of every month.

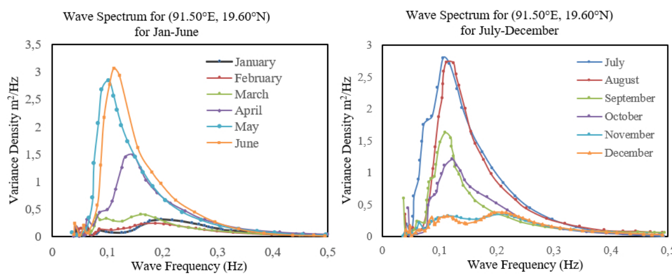

Source: Authors.

Figure 4: Location of the present study.

Source: Authors.

3.4. *Current at the Selected Location.*

Data on sea currents have been obtained from INCOIS [28], which serves as the central repository for marine data in India. Zonal current values around the specific region are available daily from 2022 to 2023. For each month, the maximum current values are determined. Then, the average of these monthly maximum values is calculated over the two-year period and these values are presented in Fig. 5. The current and wave direction are considered as the same for amplified motion.

Figure 5: Average of max. current speeds over two years.

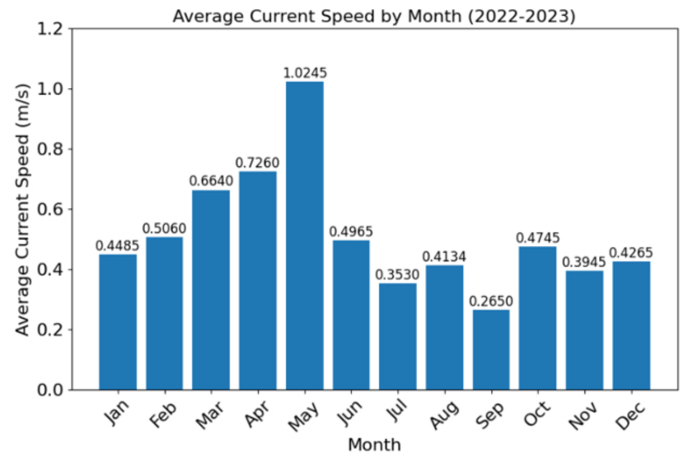

Source: INCOIS [28].

4. Results and Discussions.

4.1. *Frequency Domain Simulation.*

Figure 6 presents the comparative RAO analysis of the CS50 MK II and the traditional four-column semisubmersible. As shown, the surge, heave, and pitch responses of both structures follow similar trends, though their peak magnitudes and corresponding frequencies differ. This discrepancy may arise from their differing length and breadth dimensions, despite sharing identical displacement and draft.

Notably, the CS50 MK II exhibits lower peak magnitudes in heave and pitch motions, demonstrating superior performance in mitigating these responses across various wave frequencies. These results indicate that the CS50 MK II is a highly adaptable platform, combining enhanced mobility for relocation with improved stability in high-frequency wave conditions.

4.2. *Time domain simulation.*

The initial transient response duration is observed to be less than 3,000 seconds in all cases. The present analysis focuses on steady-state motion responses for surge, heave and pitch modes as presented in Figs. 7a, 7b and 7c respectively.

4.2.1. *Surge Motion.*

The standard deviation of linear horizontal motion (surge) reveals key differences between the CS50 MK II and the traditional four-column semisubmersible:

- Head Sea Conditions: The CS50 MK II exhibits significantly lower surge motion, attributed to its streamlined design.
- Beam Sea Conditions: The CS50 MK II shows higher surge motion than the traditional semisubmersible, likely

due to its asymmetrical structure, whereas the symmetrical design of the conventional platform ensures more consistent performance.

- Peak Deviations by Month: For CS50 MK II, maximum standard deviation occurs in April (beam sea) and July (head sea), whereas for traditional Semisubmersible, peak deviation is observed in August.

4.2.2. Heave Motion.

Heave motion remains relatively unaffected by wave heading changes. However, monthly variations are notable:

- CS50 MK II: Peak standard deviation occurs in September.

- Traditional Semisubmersible: Maximum deviation is observed in July.

4.2.3. Pitch Motion.

Pitch motion is negligible in beam sea conditions for both designs. The traditional semisubmersible exhibits higher pitch motion, with peak standard deviation occurring in July for both types.

4.2.4. Seasonal Influence of Wave Energy Spectrum.

The motion responses of the semisubmersibles may be correlated with variations in wave energy spectra as shown in Fig. 3.

- April–September: Wave energy peaks, leading to higher motion deviations (evident in Figs. 7a∼7c).

- September–February: The wave spectrum is broader but lower in magnitude, resulting in more irregular wave patterns. During this period, the CS50 MK II outperforms the traditional semisubmersible.

These findings highlight the importance of selecting a semisubmersible design based on the wave conditions of the operational region.

Conclusions.

This paper presents a comparative numerical study of motion responses between the CS50 MK II—a highly efficient and widely adopted semisubmersible design—and a conventional four-column semisubmersible in the Bay of Bengal. Both frequency-domain and time-domain analyses were conducted, incorporating site-specific wave characteristics and current conditions.

Figure 6: RAO analysis of the semisubmersibles.

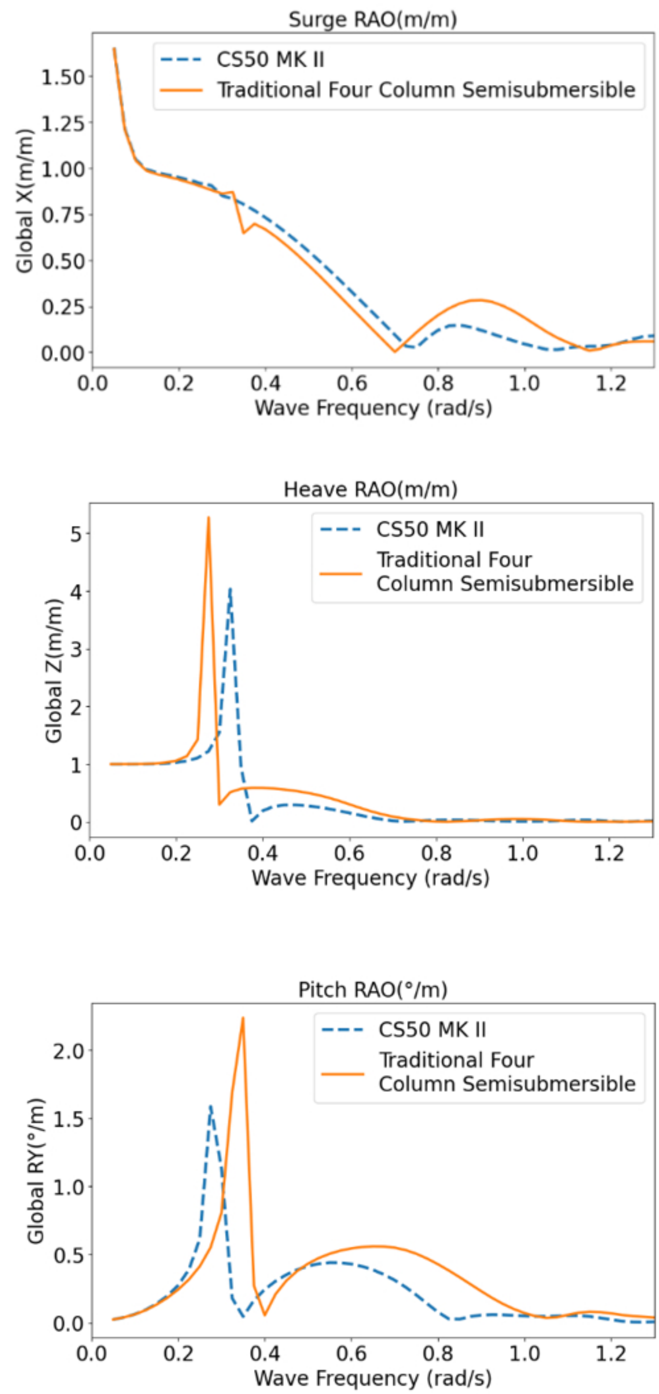

Source: Authors.

The RAO analysis for surge, heave and pitch motion exhibit similar trends for both the semisubmersibles. On the contrary, the maximum magnitude of the motion amplitudes is higher for traditional type than the CS50 MK II type. The standard deviation of surge motion is same in the head sea and beam sea condition for the traditional semi-submersible case, however it is higher in the beam sea than the head sea for CS50 MK II. The maximum standard deviation considering beam sea and head sea condition occur in the month of April and July respectively for CS50 MK II. On the other hand, for traditional semisubmersible the maximum standard deviation is observed during August. It is observed that heave motion is not affected significantly due to the change of wave headings for both the semisubmersibles. For CS50 II, the maximum standard deviation for heave motion occurs in the month of September. On the other hand, for traditional type the maximum standard deviation for heave is observed during July. It is observed that pitch motion is not observed for both the types in the beam sea condition. The standard deviation for pitch motion is higher for traditional type. The maximum standard deviation for pitch motion occurs in the month of July for the types.

While this numerical study provides valuable insights into motion characteristics under the Bay of Bengal wave conditions, no definitive conclusion can be drawn regarding superior performance, since motion response is just one critical parameter among many. Based on the present study, future research can focus on experimental validation of numerical models, advanced simulations incorporating coupled dynamics, design optimization for region-specific conditions and cost-benefit analyses and operational strategy refinements. This work establishes a foundational understanding to guide further innovation in semisubmersible design, ensuring robust performance across diverse marine environments.

References.

[1] Sajid, E.,2022, "We have gas reserve for 10 years only – then what? " The Business Standard, Retrieved June17, 2025, from https://www.tbsnews.net/bangladesh/energy/we-have-gas-reserve-10-years-only-then-what-405470

[2]Annual report 2022-23, Bangladesh Oil, Gas and Mineral Corporation (Petrobangla)

[3] Seam, N. M. and Ami, R. A., 2021, "The Bay of Bengal: the embryonic energy source for Bangladesh economy." The Business Standard. Retrieved June17, 2025, from https://www.researchgate.net/publication/351599005_The_Bay_of_Bengal_the_embryonic_e

[4] Sajid, E. and Siddiqui, K., 2022, "Big potential in Bay as 17-103 TCF gas hydrates found," The Business Standard, Retrieved June17, 2025, from https://www.tbsnews.net/bangladesh/gas-hydrate-found-bay-bengal-353539

[5] Sarhan, O. and Raslan, M., 2021, "Offshore petroleum rigs/platforms: An overview of analysis, design, construction, and installation, " International Journal of Advanced Engineering Sciences and Applications, 2(1), 58.

[6] Ruzanna, A. B., 2012, "Computer-aided design of semi-submersible for deepwater operations, " Department of Mechanical Engineering, Universiti Teknologi PETRONAS.

[7] Ralha, D. C. B., Corrêa, M. C., and Pinheiro, K. G., 2019, "Mooring system for a semi-submersible rig in ultra-deepwater and under severe currents, " Journal of Marine Structures, 63, 120-131.

[8] Patra, A., Bhaskaran, P. K., and Maity, R., 2019, "Spectral wave characteristics over the Head Bay of Bengal: A modeling study, " Ocean Dynamics, 69(10), 1233-1245.

[9] Wu, L., Zhang, C., and Zhao, X., 2017, "Simplified algorithm for evaluating hydrodynamic performance of mobile offshore base, " Marine Technology Society Journal, 51(2), 108-120.

[10] Ng, C. Y., and Tahar, R., 2011, "Experimental investigation for the responses of semi-submersible platform subjected to bidirectional waves, " Journal of Ocean Engineering, 38(17-18), 2149-2158.

[11] Qiao, D., and Ou, J., 2013, "Global responses analysis of a semi-submersible platform with different mooring models in the South China Sea, " Marine Structures, 32, 117-136.

[12] Chuang, Z., Zhang, W., and Wang, Z., 2022, "Dynamic performance optimization of an arctic semi-submersible production system, " Ocean Engineering, 242.

[13] Alimuddin, M., and Islam, M. R., 2017, "Prediction of motion of a semi-submersible, " Procedia Engineering, 194, 144-151.

[14] Liu, Y., Zhang, H., and Wu, Y., 2015, "Numerical investigation on interaction between a semi-submersible platform and its mooring system, " Journal of Offshore Mechanics and Arctic Engineering, 137(4).

[15] Zan, Y., Zhang, J., and Liu, Y., 2023, "Advanced prediction models for mooring tension, " Ocean Engineering, 266.

[16] Uwihanganye, B., Musial, W., and Mapes, M., 2018, "Numerical approaches in the optimization of mooring systems for floating structures, " International Journal of Engineering Technology and Scientific Innovation, 1(2), 45-62.

[17] Sanni, A., and Olusegun, O., 2012, "Analysis of mooring systems for offshore vessels in deep waters, " Ocean Engineering, 60, 63-73.

[18] Zhao, W., Wang, C., and Liu, Y., 2022, "Numerical simulations of vortex-induced motions of a semi-submersible, " Ocean Engineering, 249.

[19] Hamn-Ching, C., and Li, J., 2016, "Simulation of vortex-induced motions of a deep draft semi-submersible in current, " Journal of Fluid Mechanics, 801, 1-20.

[20] Vamshikrishna, D., and Rajiv, S., 2020, "An experimental study on vortex-induced motion responses of a moored semi-submersible with and without riser, " Ocean Engineering, 207, 107365.

[21] Rodolfo, M., and Hamza, R., 2012, "Experimental study on vortex-induced motions of a semi-submersible platform with four square columns, " Journal of Fluids and Structures, 35, 116-134.

[22] Yongpyo, K., and Hanseong, K., 2008, "Experimental study on the global motion performance of deep-draft semi-submersibles

in wind, wave, and current environments, " Journal of Offshore Mechanics and Arctic Engineering, 130(4), 041101.

[23] Agroza, D., Arvidsson, S., and Ljungberg, M., 2023, "Offshore facilities for hydrate extraction in the Bay of Bengal: Platform selection based on sedimentation and water depth, " Journal of Marine Engineering.

[24] Ove, T., and Daniel, S., 2021, "Floating structural concepts and riser systems for deep and ultra-deep water for East Coast of India, " International Journal of Offshore and Polar Engineering, 31(1).

[25] 2008 Worldwide survey of deepwater drilling rigs, Offshore Magazine, Retrieved June17, 2025, from https://oilproduction.net/fi

000-2008%20drillrig-posterfinal-app.pdf

[26] Ali, M. T., 2021, "A Numerical Investigation on Hydrodynamic Interaction Coefficients for a Group of Truncated Composite Cylinders Floating in Waves." 40th International Conference on Ocean, Offshore and Arctic Engineering, OMAE2021-63037.

[27] GRABCAD COMMUNITY, Retrieved June17, 2025, from https://grabcad.com/library/moss-cs50-mkii-oil-platform.

[28] ESSO, Indian National Centre for Ocean Information Services, Retrieved June17, 2025, from https://incois.gov.in/

Appendix.

Figure 7: Variation of standard deviation for surge with wave heading and months.

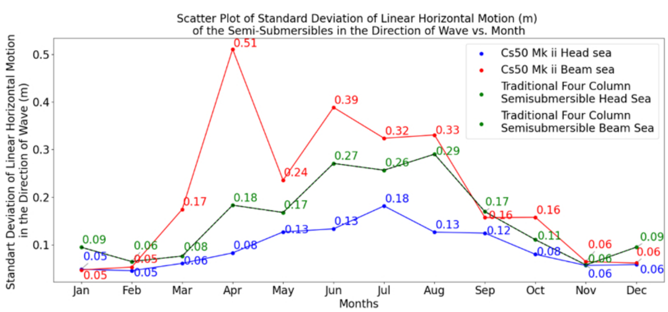

Source: Authors.

Figure 8: Variation of standard deviation for surge with wave heading and months.

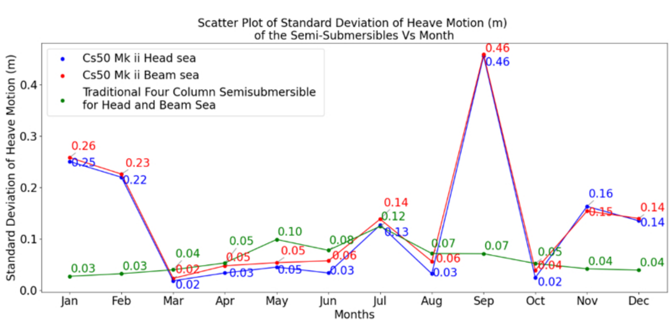

Source: Authors.

Figure 9: Variation of standard deviation for heave with wave heading and months.

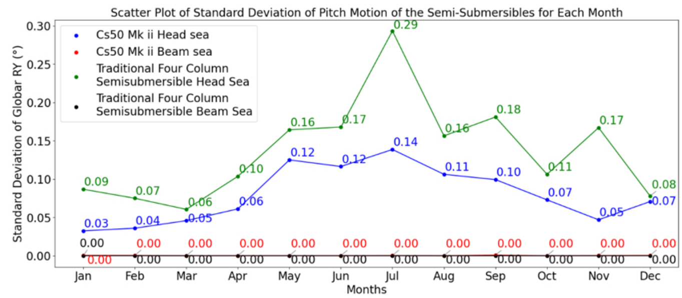

Source: Authors.